MOLECULAR AND CELLULAR BIOLOGY, July 1992, p. 2986–2996
0270-7306/92/072986-11$02.00/0

Vol. 12, No. 7

The Rate-Limiting Step in Yeast *PGK1* mRNA Degradation Is an Endonucleolytic Cleavage in the 3′-Terminal Part of the Coding Region

PETER VREKEN AND HENDRIK A. RAUÉ*

Faculty of Chemistry, Department of Biochemistry and Molecular Biology, Vrije Universiteit de Boelelaan 1083, 1081 HV Amsterdam, The Netherlands

Received 11 December 1991/Accepted 14 April 1992

Insertion of an 18-nucleotide-long poly(G) tract into the 3′-terminal untranslated region of yeast phosphoglycerate kinase (*PGK1*) mRNA increases its chemical half-life by about a factor of 2 (P. Vreken, R. Van der Veen, V. C. H. F. de Regt, A. L. de Maat, R. J. Planta, and H. A. Raué, Biochimie 73:729–737, 1991). In this report, we show that this insertion also causes the accumulation of a degradation intermediate extending from the poly(G) sequence down to the transcription termination site. Reverse transcription and S1 nuclease mapping experiments demonstrated that this intermediate is the product of shorter-lived primary fragments resulting from endonucleolytic cleavage immediately downstream from the U residue of either of two 5′-GGUG-3′ sequences present between positions 1100 and 1200 close to the 3′ terminus (position 1251) of the coding sequence. Similar endonucleolytic cleavages appear to initiate degradation of wild-type *PGK1* mRNA. Insertion of a poly(G) tract just upstream from the AUG start codon resulted in the accumulation of a 5′-terminal degradation intermediate extending from the insertion to the 1100–1200 region. RNase H degradation in the presence of oligo(dT) demonstrated that the wild-type and mutant *PGK1* mRNAs are deadenylated prior to endonucleolytic cleavage and that the half-life of the poly(A) tail is three- to sixfold lower than that of the remainder of the mRNA. Thus, the endonucleolytic cleavage constitutes the rate-limiting step in degradation of both wild-type and mutant *PGK1* transcripts, and the resulting fragments are degraded by a 5′→3′ exonuclease, which appears to be severely retarded by a poly(G) sequence.

Over the past decade, it has become evident that the pattern of gene expression in a cell is determined not only by factors controlling transcription but to a large extent also by posttranscriptional events, including the rate of degradation of the individual mRNAs. In both prokaryotic and eukaryotic cells, different mRNAs show sometimes considerable differences in stability that are of fundamental importance in establishing their relative cellular levels. Furthermore, there are numerous examples of adjustments in the half-life of particular mRNAs in response to specific stimuli that play a major role in the adaptation of the cells to changing conditions (for recent reviews, see references 1, 4, 9, 12, and 48).

To gain more insight into the manner in which turnover of their transcripts contributes to the control of expression of particular genes, considerable effort is being put into the characterization of structural features within mRNA governing the rate of decay, as well as the *trans*-acting factors involved. As a result, a number of structural determinants of prokaryotic as well as eukaryotic mRNA stability have now been identified. Among the eukaryotic stability determinants so far characterized are the AU-rich sequences responsible for the rapid turnover of a group of mRNAs encoding lymphokines, interferons, and cellular growth factors (13, 46, 49, 50), the stem-loop structure at the 3′ terminus of mammalian histone mRNAs that governs their cell cycle-dependent destabilization (35, 42), and the iron-responsive elements, a cluster of hairpins that is located in the 3′-terminal untranslated region (3′-UTR) of the transferrin receptor mRNA and controls changes in the stability of this transcript in response to the intracellular iron concentration (14, 38, 57). In other cases, evidence for defined, but not yet fully characterized, *cis*-acting stability determinants has been obtained (8, 19, 23, 26, 27, 43, 47, 50, 51, 64, 65). In addition more general properties of messengers such as their ability to be completely translated (2, 3, 15–17, 21, 24, 29, 32, 43, 44) and their polyadenylation (1, 5, 9, 40) have been found to influence stability.

Recently progress has also been made in the identification of *trans*-acting factors involved in eukaryotic mRNA decay. These include a nucleoprotein interacting with the AU-rich sequences (10, 11), which may be part of a family of AU-binding factors (7, 33, 58), and a protein that interacts with the iron-responsive elements of the transferrin receptor mRNA (28, 39). Furthermore, histones as well as β-tubulin were shown to control turnover of their respective mRNAs by a feedback mechanism (45, 66, 67). Despite this expansion in our knowledge of *cis*- and *trans*-acting stability determinants, however, the details of eukaryotic mRNA turnover are still only poorly understood. In particular, little is yet known concerning the nature of the targets at which degradation is initiated or about the nucleases involved in the decay process.

In yeast cells, mRNA half-lives vary from 1 to about 100 min (12, 19). Thus, yeast mRNAs constitute an excellent set of molecules with which to identify and study factors governing mRNA stability. Moreover, the genetic and molecular biological advantages of yeast cells compared with mammalian cells should considerably facilitate the unraveling of the mechanism(s) of mRNA degradation (37). Studies on turnover of specific yeast mRNAs, however, have so far provided only limited information, mainly concerning *cis*-acting (de)stabilizing elements (19, 43, 62). Several yeast endo- and exoribonucleases have been identified (52–55), but a role for

* Corresponding author.

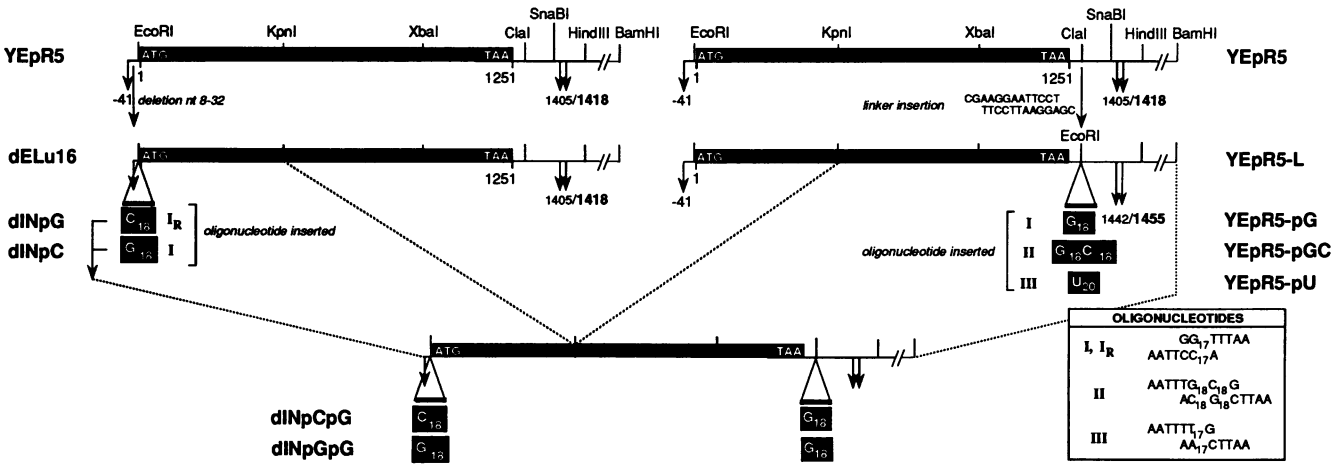

FIG. 1. Schematic representation of the construction of the *PGK1*-carrying plasmids used in this study. The black bar represents the *PGK1* coding region. Arrows correspond to the transcription initiation and termination sites determined previously (59, 62). The major site of transcription termination (present in approximately 80% of the transcripts; see Fig. 4) is indicated in boldface. The coordinates are relative to the translation start site. YEpR5-L was obtained by inserting a synthetic deoxyoligonucleotide containing an *Eco*RI site into the *Cla*I site present in the 3′-UTR of YEpR5. Various synthetic deoxyoligonucleotides were subsequently inserted into the resulting *Eco*RI site to obtain YEpR5-pG, -pGC, and -pU. The oligonucleotides used are shown in the box at the lower right. In all cases, the insertion restored a single *Eco*RI site downstream from the inserted sequence. dINpG and dINpC were obtained by inserting the same deoxyoligonucleotide in either orientation (I or I_R) into the *Eco*RI site just upstream of the ATG start codon of plasmid dELu16. The latter was derived from YEpR5 by deleting nt 8 to 32 from the 5′-UTR (60). Restriction sites used in the construction of the various mutant genes are shown.

these enzymes in mRNA degradation has not yet been documented.

In a previous study from our laboratory (62), we showed that the half-life of the yeast phosphoglycerate kinase (*PGK1*) mRNA can be increased about twofold by insertion of an 18-nucleotide (nt)-long poly(G) stretch into the 3′-UTR. In this report, we present experiments on the mechanism of degradation of *PGK1* mRNA evolving from the observation that this insertion causes the accumulation of a 3′-terminal fragment of the *PGK1* transcript, while insertion of a similar poly(G) tract into the 5′-UTR results in the accumulation of a 5′-terminal fragment. We show that these fragments are due to specific rate-limiting endonucleolytic cleavage near the 3′ end of the *PGK1* coding region, after previous deadenylation of the transcript. The cleavage products appear to be removed primarily by 5′→3′ exonucleolytic degradation, which is retarded by the presence of the poly(G) sequence. The same mechanism appears to operate for wild-type *PGK1* mRNA. Since poly(G) barriers are absent in this case, however, no degradation products accumulate.

MATERIALS AND METHODS

Enzymes and deoxyoligonucleotides. Restriction enzymes were obtained from either Bethesda Research Laboratories (Gaithersburg, Md.) or New England Biolabs (Beverly, Mass.) and used according to the supplier's instructions. The Klenow fragment of DNA polymerase I, S1 nuclease, polynucleotide kinase, and Moloney murine leukemia virus reverse transcriptase were from Bethesda Research Laboratories. Radiolabeled nucleotides were obtained from Amersham (Amersham, United Kingdom). Synthetic deoxyoligonucleotides were prepared in our laboratory by using an Applied Biosystems 381A DNA synthesizer.

Strains and plasmids. Construction of the plasmids used in this study is schematically depicted in Fig. 1. A detailed description of the construction of dINpG and YEpR5-pG, which carry a *PGK1* gene containing an 18-nt-long poly(G) insertion in the 5′-UTR (dINpG) or the 3′-UTR (YEpR5-pG), has been published elsewhere (59, 60, 62). Plasmid dINpGpG, containing a *PGK1* gene that carries a poly(G) tract in both UTRs, was constructed by replacing the *Kpn*I-*Bam*HI fragment of dINpG by the corresponding fragment from YEpR5-pG. Plasmid dINpCpG is identical to dINpGpG except that it contains a poly$(C)_{18}$ instead of a poly$(G)_{18}$ insertion in the 5′-UTR. It was obtained by replacing the *Kpn*I-*Bam*HI fragment of dINpC (60) by the corresponding fragment from YEpR5-pG. *Saccharomyces cerevisiae* 20B-12 (*trp1 pep4-3* [25]) and Y260 (*MAT***a** *ura3-52 rpb1-1*), which contains a temperature-sensitive RNA polymerase II (41), were used as hosts for episomal vectors carrying mutant *PGK1* genes. Transformants were grown in minimal medium at 24°C (Y260) or 30°C (20B-12). Temperature shift from 24 to 37°C of Y260 cultures to arrest transcription by RNA polymerase II was performed as described previously (62).

Isolation and purification of RNA. Total RNA was isolated from yeast transformants according to Zitomer et al. (69). Isolation of poly$(A)^+$ and poly$(A)^-$ RNA was performed on oligo(dT) columns (Stratagene) as described by Maniatis et al. (34). Size fractionation of poly$(A)^-$ RNA for further characterization of the degradation intermediates was carried out by centrifugation through 10 to 30% linear sucrose gradients in 10 mM Tris-HCl (pH 7.4)–100 mM NaCl–1 mM EDTA for 3 h at 41,000 rpm in a Beckman SW41 rotor at 4°C. Fractions of 1 ml were taken and analyzed for the presence of *PGK1* transcripts by Northern (RNA) hybridization.

RNase H protection analysis. RNase H-directed cleavage of RNA was carried out essentially as described by Hwang et al. (22). Briefly, 10 μg of total RNA isolated at different times after transcriptional arrest was annealed to 5 ng of the appropriate deoxyoligonucleotide in 40 μl of buffer R (25 mM Tris-HCl [pH 7.5], 200 mM NaCl, 5 mM $MgCl_2$). Where indicated, 500 ng of oligo$(dT)_{12-17}$ was added. The reaction mixture was heated at 85°C for 2 min, rapidly cooled to 65°C,

and then allowed to cool slowly to 37°C. Dithiothreitol was added to a final concentration of 1 mM, and cleavage was effected by incubating the sample with 1 U of RNase H (Promega) for 45 min at 37°C. The reaction was terminated by adding 50 μl of a phenol-chloroform-isoamyl alcohol mixture (25:25:1, vol/vol/vol). RNA was precipitated from the aqueous phase with ethanol and resuspended in 10 μl of sterile H_2O.

Northern analysis, primer extension, and S1 nuclease mapping. Northern analysis was carried out by fractionating RNA samples after treatment with glyoxal (34) on 2% agarose or, in the case of small fragments, 6% Nusieve agarose (FMC) gels, followed by transfer to nylon membranes (Amersham). Hybridization with radiolabeled deoxyoligonucleotides, using the *Eco*RI-*Cla*I fragment of plasmid YEpR5 (59, 60), spanning the *PGK1* coding region or the *Taq*I-*Hpa*I fragment of plasmid pBMCY138 corresponding to the 5′-terminal two-thirds of the coding region of yeast gene encoding ribosomal protein L25 (31), was carried out in 6× SSC (1× SSC is 0.15 M NaCl plus 0.015 M sodium citrate)–5× Denhardt's solution (100× Denhardt's solution is 0.2% Ficoll, 0.2% bovine serum albumin, and 0.2% polyvinylpyrrolidone)–0.5% sodium dodecyl sulfate at either 42 or 65°C, depending on the probe. Unless indicated otherwise, hybridization experiments were carried out under conditions of excess probe. Probes were either end labeled with [γ-^{32}P]ATP (34) or labeled with [α-^{32}P]ATP by means of a random-priming kit obtained from Promega. Primer extension and S1 nuclease mapping experiments were carried out as described previously (62).

RESULTS

Accumulation of a 3′-terminal degradation intermediate in cells transformed with *PGK1* genes carrying an altered 3′-UTR. We have previously analyzed the effects of homo- and heteropolymer insertions into the 5′- and 3′-UTR of yeast *PGK1* mRNA on the half-life of the transcript by means of Northern analysis, after transcriptional arrest, using a probe complementary to the 5′-terminal part of the coding region (62). In accordance with in vivo studies on the degradation of other, prokaryotic as well as eukaryotic mRNAs, we did not detect any products shorter than the intact transcript, indicating that as a rule, intermediates formed during mRNA degradation are extremely short-lived. However, when we repeated these experiments using a deoxyoligonucleotide (designated TPGK, for trailer of *PGK1* gene) complementary to part of the 3′-UTR (nt 1337 to 1353), we did observe significant amounts of a fragment with an estimated size of about 180 nt in Y260 cells transformed with *PGK1* genes that carry either an 18-nt-long poly(G) tract (*PGK1*-pG) (YEpR5-pG; Fig. 2A, lane 3) or the same tract followed by poly$(C)_{18}$ (*PGK1*-pGC) (YEpR5-pGC; Fig. 2A, lane 2) in the 3′-UTR (see Fig. 1). As shown previously, the half-lives of the *PGK1*-pG and *PGK1*-pGC transcripts are increased by about 70 and 25%, respectively, over that of their wild-type counterparts (62). The accumulation of the 3′-UTR-derived product, however, does not appear to be directly correlated with increased metabolic stability of the transcript, since insertion of a 20-nt-long poly(U) tract into the 3′-UTR, which has approximately the same effect on *PGK1* mRNA stability as does the poly(G) insertion (62), does not cause the appearance of a comparable product (YEpR5-pU; Fig. 2A, lane 4). Moreover, we could not detect such a product in control cells transformed with the wild-type gene (YEpR5; Fig. 2A, lane 1) or in cells expressing any of the other trailer insertion

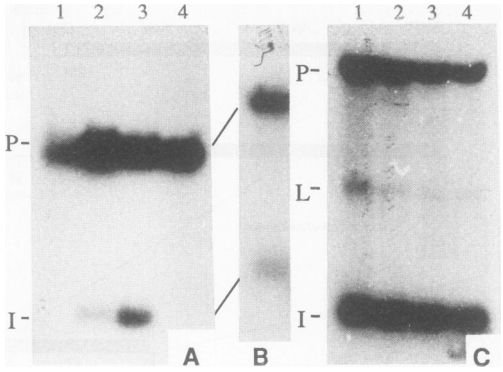

FIG. 2. Detection of a 3′-terminal intermediate formed during degradation of mutant *PGK1* mRNA. (A) Ten micrograms of total RNA isolated from Y260 cells transformed with multiple copies of mutant *PGK1* genes carrying different insertions into the 3′-UTR (see Fig. 1) and grown to mid-log phase at 24°C was subjected to Northern analysis with an excess of the trailer-specific TPGK deoxyoligonucleotide radiolabeled at its 5′ end. Lanes: 1, YEpR5-derived mRNA; 2, YEpR5-pGC-derived mRNA; 3, YEpR5-pG-derived mRNA; 4, YEpR5-pU-derived RNA. (B) Similar Northern analysis of total RNA isolated from exponentially growing 20B-12 cells transformed with plasmid YEpR5-pG. (C) Time course of degradation of intact YEpR5-pG mRNA and the degradation intermediate after transcriptional arrest. YEpR5-pG-transformed cells were subjected to transcriptional arrest by raising the temperature of the culture from 24 to 37°C. Total RNA was isolated at various times thereafter and analyzed by Northern hybridization using an excess dC deoxyoligonucleotide, radiolabeled at its 5′ end, as well as the *Taq*I-*Hpa*I fragment of the yeast ribosomal protein L25 gene, radiolabeled by random priming as probes (62). The bands were quantified by laser scanning densitometry (60, 62) at 0 min (lane 1), 20 min (lane 2), 40 min (lane 3), and 60 min (lane 4) after transcriptional arrest. The intact *PGK1*-pG and L25 transcripts and the 3′-terminal degradation intermediate are indicated by P, L, and I, respectively.

mutants (60) of the *PGK1* gene (data not shown). On the other hand, the accumulation of the 3′-UTR-derived product is not due to some peculiarity of strain Y260, which carries a temperature-sensitive mutation in the gene encoding the largest subunit of RNA polymerase II (41). As shown in Fig. 2B, the same product is clearly observed in exponentially growing 20B-12 cells transformed with plasmid YEpR5-pG. The relative amount of the intermediate in this case is lower than in Y260 cells, which may be due to the higher growth rate of 20B-12 cells.

Figure 2C shows the results of a Northern analysis carried out on total RNA isolated from YEpR5-pG-transformed Y260 cells at various times after arrest of transcription by an increase in growth temperature from 24 to 37°C, which inactivates RNA polymerase II in these cells (41). The amount of the 180-nt-long fragment does not decrease by more than about 15% (as determined by optical scanning of the autoradiogram) over a period of 60 min, while intact *PGK1*-pG mRNA and ribosomal protein L25 mRNA disappear at rates in accordance with their previously determined half-lives (62). These results are consistent with a precursor-product relationship between the intact *PGK1* transcript and the fragment, with the half-lives of the two molecules being approximately equal. Unfortunately, as a result of cell death, mRNA decay can not be monitored for periods longer than about 90 min, thus precluding direct measurement of the half-life of the fragment. Since in this experiment a deoxyoligonucleotide complementary to the poly(G) insertion, des-

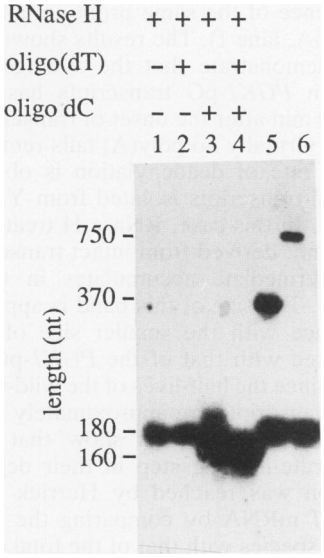

FIG. 3. Analysis of poly(A) tail length of the 3′-terminal degradation intermediate. Total RNA was isolated from YEpR5-pG-transformed Y260 cells growing exponentially at 24°C, annealed to different deoxyoligonucleotides as indicated, and subsequently incubated with RNase H. Cleavage products were analyzed by Northern hybridization with excess 3′-UTR-specific TPGK deoxyoligonucleotide, radiolabeled at the 5′ end (lanes 1 to 4). Lanes 5 and 6 contain size markers obtained by RNase H cleavage of *PGK1*-pG mRNA after annealing to deoxyoligonucleotides complementary to either nt 1024 to 1049 (lane 5) or nt 640 to 665 (lane 6).

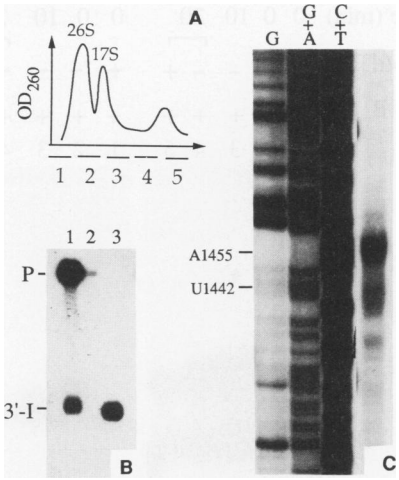

FIG. 4. Mapping of the 3′ terminus of the degradation intermediate. Poly(A)$^-$ RNA was isolated from exponentially growing YEpR5-pG-transformed Y260 cells and fractionated on a 10 to 30% sucrose density gradient. Fractions were pooled as indicated in panel A, which shows the OD_{260} (optical density at 260 nm) profile of the gradient. (B) Northern analysis of various fractions with the trailer-specific TPGK deoxyoligonucleotide as the probe. Lanes: 1, total poly(A)$^-$ RNA (10 μg); 2, fraction 4 (5 μg); 3, fraction 5 (0.5 μg). (C) S1 nuclease analysis of the RNA present in fraction 5, using the *Eco*RI-*Hin*dIII fragment, labeled at the *Eco*RI site, of the *PGK1*-pG gene as the probe (see Fig. 1). P, intact *PGK1*-pG transcript; 3′-I, 3′-terminal degradation intermediate.

ignated dC [complementary to the region of the 3′-UTR that includes the poly(G) tract as well as 4 nt upstream and 1 nt downstream from this tract], was used as the probe, we conclude that the trailer-derived fragment still contains most, if not all, of the poly(G) tract. The poly(G) insertion, thus, not only increases the metabolic stability of the intact *PGK1*-pG transcripts (62) but also alters the structure of its 3′-UTR in such a way that it is less susceptible to further degradation by the nucleolytic enzymes involved in removing mRNA fragments.

Further characterization of the 3′-terminal degradation intermediate. The presence of the poly(G) tract in the 3′-UTR-derived fragment, together with its estimated length, indicates that the fragment contains most, if not all, of the original 3′ untranslated sequence and does not carry a poly(A) tail of any significant length. To establish the absence of a poly(A) tail directly, we annealed total RNA from exponentially growing YEpR5-pG-transformed Y260 cells to oligo(dT) and treated the resulting hybrids with RNase H. Products were analyzed by Northern hybridization with the 3′-UTR-specific TPGK deoxyoligonucleotide as the probe. Since the RNase H treatment does not detectably change the size of the degradation intermediate (Fig. 3; compare lanes 1 and 2), we conclude that this fragment indeed contains at most only a few A residues at its 3′ end. When RNase H cleavage was carried out in the presence of the dC deoxyoligonucleotide, a product with a length of approximately 160 nt was obtained, accompanied by a smear at its upper end which must represent poly(A) tails present on intact *PGK1*-pG transcripts (Fig. 3, lane 3). This conclusion is confirmed by the fact that the smear disappeared when cleavage was carried out in the presence of both the dC deoxyoligonucleotide and oligo(dT) (Fig. 3, lane 4).

The difference in length between the original intermediate and the product resulting from its cleavage by RNase H in the presence of the dC deoxyoligonucleotide indicates that the 5′ end of the degradation intermediate is located at, or at least very close to, the 5′ end of the poly(G) tract of the *PGK1*-pG transcript. Attempts to map the 5′ end more precisely by primer extension analysis failed because the reverse transcriptase proved to be unable to transcribe through a poly(G) sequence.

To identify the 3′ terminus of the degradation intermediate precisely, we separated poly(A)$^-$ RNA isolated from YEpR5-pG-transformed Y260 cells on a 10 to 30% linear sucrose density gradient (Fig. 4A). Northern analysis (Fig. 4B) shows the top fraction of this gradient to contain virtually all of the intermediate and to be devoid of intact transcript. This fraction was then used in an S1 nuclease mapping experiment with the *Eco*RI-*Hin*dIII fragment of the YEpR5-pG-encoded *PGK1*-pG gene, labeled at the *Eco*RI site, as the probe [see Fig. 1; note that the *Eco*RI site is located downstream from the poly(G) insertion]. The results (Fig. 4C) reveal two closely spaced 3′ ends at positions 1442 and 1455 that, taking into account the length of the inserted sequence, correspond exactly to those previously determined for the intact wild-type *PGK1* transcript at positions 1405 and 1418 (62). About 80% of the 3′-UTR-derived fragments has the longer size, in accordance with the use of the site farthest downstream as the major transcription termination site (62). This result confirms that the 3′-terminal degradation intermediate extends to the transcription termination site of the gene. However, the presence of a short remnant of the original poly(A) tail cannot be excluded.

Rate of poly(A) tail shortening in wild-type *PGK1* and *PGK1*-pG mRNAs. Because removal of the poly(A) tail appears to precede the specific endonucleolytic cleavage of

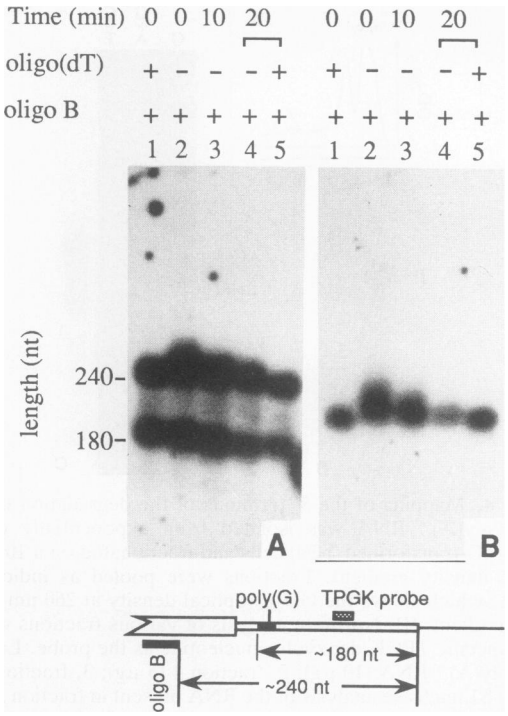

FIG. 5. Rate of deadenylation of *PGK1*-pG and wild-type *PGK1* mRNAs. Total RNA was isolated from YEpR5-pG-transformed (A) or YEpR5-transformed (B) Y260 cells at various times after transcriptional arrest, annealed to an excess of different deoxyoligonucleotides as indicated, and subsequently incubated with RNase H. The products were analyzed by Northern hybridization with an excess of the TPGK or oligo B probe, radiolabeled at the 5′ end. The diagram is a schematic representation of the 3′-terminal region of the *PGK1* gene and indicates the nature of the deoxyoligonucleotides used as well as the expected cleavage products.

PGK1-pG mRNA that gives rise to the degradation intermediate, the stabilizing effect of the poly(G) insertion might be due to a decrease in the rate of deadenylation of the mutant transcript relative to that shown by its wild-type counterpart. Therefore, we compared the rates at which the poly(A) tail is removed from the two types of transcript. Total RNA was isolated from YEpR5-pG- as well as YEpR5-transformed Y260 cells at various times after transcriptional arrest and treated with RNase H in the presence of a deoxyoligonucleotide complementary to nucleotides 1165 to 1217 of the *PGK1* coding region (oligo B). In the case of YEpR5-pG transformants (Fig. 5A), the Northern analysis of the cleavage products, using the trailer-specific TPGK probe, reveals the presence of two bands. The lower band corresponds to the 180-nt-long degradation intermediate described above, which is not affected by the RNase H treatment. The upper band shows a length of about 240 nt, corresponding to the distance between the downstream end of the RNase H probe (position 1217) and the major transcription termination site of the *PGK1*-pG gene. This product must be derived from intact, deadenylated *PGK1*-pG transcripts that are present at a relatively high level in the exponentially growing transformants (Fig. 4B). Polyadenylated *PGK1*-pG transcripts are represented by the diffuse hybridization signal trailing the 240-nt-long band (Fig. 5A, lane 2). This conclusion was confirmed by the disappearance of this diffuse signal when RNase H treatment was carried out in the presence of the same probe in combination with oligo(dT) (Fig. 5A, lane 1). The results shown in lanes 3 and 4 of Fig. 5A demonstrate that the average length of the poly(A) tails on *PGK1*-pG transcripts has decreased by about 50% at 10 min after the onset of transcriptional arrest, while at 20 min virtually no poly(A) tails remain detectable. A very similar rate of deadenylation is observed for the wild-type *PGK1* transcripts isolated from YEpR5 transformants (Fig. 5B). In this case, RNase H treatment produces only a single band, derived from intact transcripts, since no degradation intermediate accumulates in these transformants (Fig. 2A). The size of this band is approximately 210 nt, in accordance with the smaller size of the wild-type 3′-UTR compared with that of the *PGK1*-pG mutant transcript (Fig. 1). Since the half-lives of the wild-type *PGK1* and the *PGK1*-pG transcripts are approximately 34 and 60 min, respectively (62), these results show that deadenylation cannot be the rate-limiting step in their degradation. The same conclusion was reached by Herrick et al. (19) for wild-type *PGK1* mRNA by comparing the half-life of the polyadenylated species with that of the total cellular pool of *PGK1* transcripts. Therefore, the half-life of wild-type *PGK1* mRNA as well as its counterparts carrying a mutant 3′-UTR must be determined by the rate at which specific endonucleolytic cleavage of the transcripts takes place. This step appears to be retarded by particular modifications of the 3′-UTR.

Localization of the endonucleolytic cleavage sites in *PGK1*-pG mRNA. The 3′-terminal degradation intermediate identified in YEpR5-pG-transformed cells might be the primary product of endonucleolytic cleavage. Alternatively, it might accumulate because of the presence of the poly(G) tract at its 5′ end but in fact be a fragment of a larger product arising from cleavage at a site farther upstream from the insertion. To determine the location of the endonucleolytic target site, we performed primer extension analysis on poly(A)$^-$ RNA isolated from exponentially growing YEpR5-pG-transformed Y260 cells. According to the conclusion drawn from data presented above, this poly(A)$^-$ RNA should be enriched in primary degradation intermediates. To discriminate between nonspecific stops and actual 5′ ends, we used poly(A)$^+$ RNA from the same cells, which should contain only intact *PGK1*-pG mRNA molecules, as a control. Reverse transcription analysis of the two RNA fractions, using the dC deoxyoligonucleotide as the primer, is presented in Fig. 6A. Two major specific stops are visible at G-1147 and G-1180 located in the coding region of the gene, which extends to position 1251. Strikingly, both positions correspond to the 3′-terminal nucleotide of a 5′-GGUG-3′ sequence motif (Fig. 7).

If the 5′ ends at G-1147 and G-1180 are the direct result of endonucleolytic cleavage, RNA fragments with 3′ ends mapping just upstream from these positions should be present. Therefore, we performed an S1 nuclease mapping experiment on poly(A)$^-$ RNA isolated from YEpR5-pG-transformed Y260 cells, using the *Xba*I-*Eco*RI fragment (nt 952 to 1302) of the *PGK1*-pG gene, labeled at the *Xba*I site, as the probe (Fig. 1). Initial experiments failed to reveal any 3′ ends, probably because we could not add sufficient probe to arrive at an excess over the large amount of intact deadenylated *PGK1*-pG mRNA present in the poly(A)$^-$ fraction. To circumvent this problem, we analyzed the various sucrose gradient fractions shown in Fig. 4A. Figure 6B demonstrates that in this way, major bands that correspond to 3′ ends at positions G-1099, U-1130, and U-1134 can be detected. By far the highest abundance of these 3′

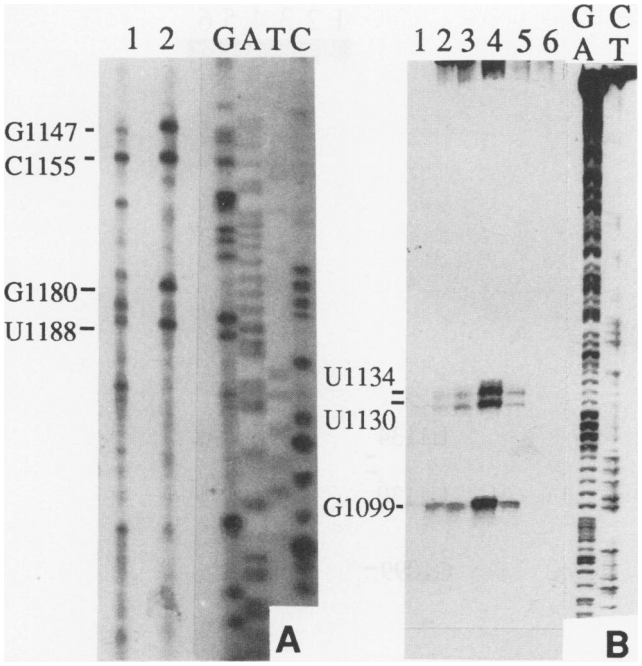

FIG. 6. Mapping of the endonucleolytic cleavage site within *PGK1*-pG mRNA. Total RNA was isolated from exponentially growing YEpR5-pG-transformed Y260 cells and separated into the poly(A)$^+$ and poly(A)$^-$ fractions. (A) Primer extension analysis. The dC deoxyoligonucleotide (10^5 cpm) was annealed to 1 μg of poly(A)$^+$ RNA (lane 1) or 10 μg of poly(A)$^-$ RNA (lane 2). Reactions were carried out with 50 U of murine leukemia virus reverse transcriptase in the presence of 1 μg of actinomycin D. The sequence ladder was obtained with the aid of the same primer and poly(A)$^+$ RNA. (B) S1 nuclease mapping of YEpR5-pG-derived poly(A)$^-$ RNA size fractionated by sucrose density centrifugation (see Fig. 4A), using the *Xba*I-*Eco*RI fragment of the *PGK1* gene, radiolabeled at the *Xba*I site, as the probe (see Fig. 1). Lanes: 1, total poly(A)$^-$ RNA (10 μg; the probe was not in excess because of the presence of intact transcript); 2 to 5, fractions 2 to 4 (2.5 μg of RNA) (lanes 2 to 4) and fraction 5 (0.5 μg of RNA) (lane 5) of the sucrose density gradient shown in Fig. 4A; 6, total RNA (10 μg) isolated from untransformed host cells. The Maxam and Gilbert sequence ladders shown in the right-hand lanes were obtained with the *Xba*I-*Eco*RI fragment of the *PGK1* gene labeled at the *Eco*RI site.

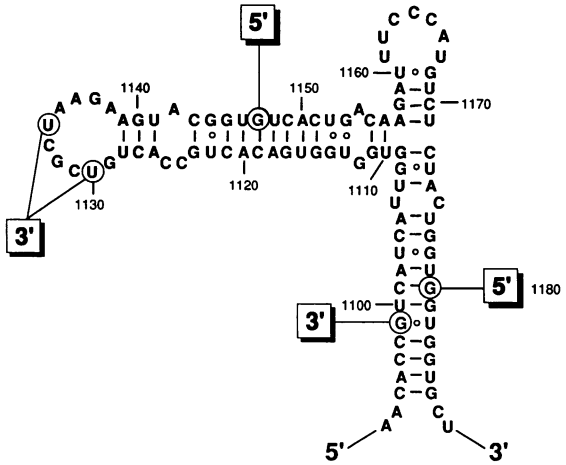

FIG. 7. Computer-generated secondary structure model of the region of *PGK1* mRNA acting as the target for endonucleolytic cleavage. The region of *PGK1* mRNA encompassing nt 1093 to 1188 together with either a 700-nt-long upstream or a 300-nt-long downstream sequence was folded by using the program FOLD (70). In the latter case, both the wild-type sequence and the mutant sequence, including the poly(G) insertion in the 3′-UTR, were analyzed. In all cases, the region from 1093 to 1188 was predicted to have the structure depicted. The 5′ and 3′ ends identified in the reverse transcription and S1 analysis shown in Fig. 6 are indicated.

termini is observed in fraction 4 of the sucrose gradient, in agreement with the expected size (~1,200 nt) of the upstream product of the endonucleolytic cleavage. Although in the primary structure of *PGK1* mRNA, the observed 3′ ends do not fit exactly to the 5′ ends at G-1147 and G-1180, in a computer-generated secondary structure model of the region in question (Fig. 7), G-1180 and G-1099 are located close to one another on either side of a double-stranded region, suggesting the involvement of a double-strand-specific endonuclease. A similar situation does not obtain, however, for the other two 3′ termini at U-1130 and U-1134, which nevertheless are reasonably close to the 5′ end at G-1147. Thus, although these results do not allow us to determine the site(s) for endonucleolytic cleavage precisely, they do support the occurrence of such specific cleavage(s) within the region of *PGK1*-pG mRNA shown in Fig. 7, close to the 3′ end of the coding sequence. The degradation intermediate accumulating in YEpR5-pG-transformed cells, therefore, is the remnant of a larger primary fragment, which seems to be rapidly trimmed by 5′→3′ exonuclease activity up to the poly(G) tract.

Accumulation of a 5′-terminal degradation intermediate in cells transformed with a *PGK1* gene carrying an altered 5′-UTR. Because insertion of a poly(G) tract into the 3′-UTR of *PGK1* mRNA stabilizes a fragment of the 3′-terminal primary degradation product, we argued that a similar insertion into the 5′-UTR might lead to the accumulation of the matching 5′-terminal intermediate that in YEpR5-pG transformants is detectable only by S1 analysis of fractionated poly(A)$^-$ RNA. Therefore, we constructed a mutant *PGK1* gene (dINpGpG; Fig. 1) containing an 18-nt-long poly(G) stretch just upstream from the AUG start codon in addition to the poly(G) insertion in the 3′-UTR. Figure 8A shows a Northern analysis of total RNA isolated from dINpGpG- and YEpR5-pG-transformed Y260 harvested during exponential growth (lanes 1 and 2, respectively). Either the trailer-specific TPGK (Fig. 8A) or the dC (Fig. 8B) deoxyoligonucleotide was used as the probe. Clearly, both mutants accumulate the same 3′-terminal degradation intermediate, albeit, for reasons that are so far obscure, not to the same level. In the dINpGpG mutant, an extra product with a size slightly below that of the intact transcript is observed which hybridizes only with the dC, not the TPGK, deoxyoligonucleotide. The same product can also be visualized by means of a randomly primed probe covering the *PGK1* coding region (Fig. 8C). The length, hybridization characteristics, and kinetics of accumulation of this fragment after transcriptional arrest (Fig. 8C) all are in agreement with the conclusion that it is the upstream product of the primary endonucleolytic cleavage in the 1100–1200 region.

Identification of the 3′ end of the 5′-terminal degradation intermediate. To ascertain that the long fragment identified above indeed originates from cleavage in the 1100–1200 region, we performed an S1 nuclease mapping experiment on poly(A)$^-$ RNA isolated from exponentially growing dINpGpG-transformed Y260 cells, using the *Xba*I-*Eco*RI

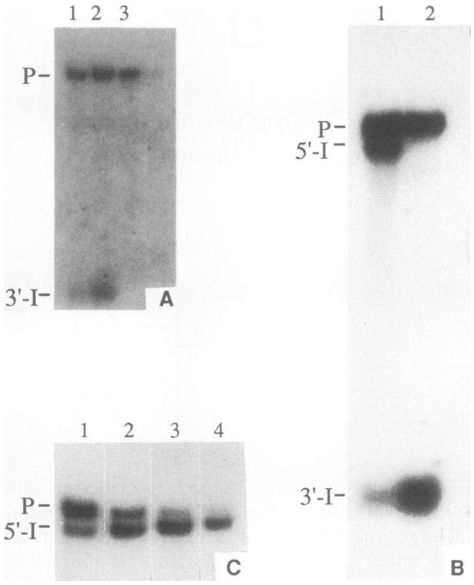

FIG. 8. Detection of a 5′-terminal degradation intermediate of *PGK1*-pGpG mRNA. Total RNA was isolated from exponentially growing Y260 cells transformed with various mutant *PGK1* genes and subjected to Northern hybridization with an excess of either the trailer-specific TPGK (A) or the dC (B) deoxyoligonucleotide probe, both radiolabeled at the 5′ end. P, intact *PGK1* transcript; 3′-I and 5′-I, 3′- and 5′-terminal degradation intermediates, respectively. Lanes: 1, dINpGpG-derived mRNA; 2, YEpR5-pG-derived RNA. Each lane contains 7.5 μg of RNA. (C) Northern analysis of total RNA isolated from dINpGpG-transformed Y260 cells at different times after transcriptional arrest. The *Eco*RI-*Cla*I fragment covering the *PGK1* coding region labeled by random priming was used as the probe. Samples were analyzed at 0 min (lane 1), 20 min (lane 2), 40 min (lane 3), and 60 min (lane 4) after transcriptional arrest.

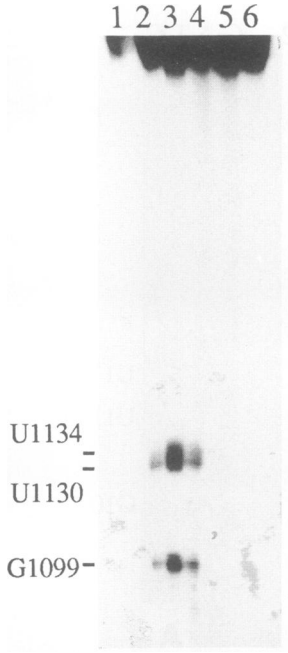

FIG. 9. Mapping of the 3′ ends of the 5′-terminal degradation intermediate derived from *PGK1*-pGpG mRNA. Total RNA was isolated from exponentially growing Y260 cells transformed with various *PGK1* mutant genes and separated into the poly(A)$^+$ and poly(A)$^-$ fractions. The latter was subjected to S1 nuclease analysis with the *Xba*I-*Eco*RI fragment of the *PGK1* gene, radiolabeled at the *Xba*I site, as the probe (see Fig. 1). Lanes: 1, YEpR5-pG-derived total poly(A)$^-$ RNA (20 μg; the probe was not in excess in this case because of the presence of intact transcript); 2, fraction 5 of YEpR5-pG-derived poly(A)$^-$ RNA (0.5 μg) fractionated by sucrose density centrifugation (see Fig. 4A); 3, dINpGpG-derived total poly(A)$^-$ RNA (20 μg; the probe was not in excess because of the presence of intact transcript); 4, dINpGpG-derived total RNA (20 μg; the probe was not in excess because of the presence of intact transcript); 5 and 6, fractions 3 and 4 of YEpR5-derived poly(A)$^-$ RNA (5 μg of each) size fractionated by sucrose gradient centrifugation in the same manner as YEpR5-pG-derived poly(A)$^-$ RNA (see Fig. 4).

fragment of the *PGK1*-pG gene, labeled at the *Xba*I site, as the probe. Figure 9 shows that 3′ ends identical to those identified in YEpR5-pG-derived RNA are readily detected even without prior fractionation (compare lanes 2 and 3). The high abundance of these 3′ ends is a clear indication that they are derived from the long 5′-terminal fragment identified above. Reverse transcription analysis of poly(A)$^-$ RNA from dINpGpG transformants, using the dC deoxyoligonucleotide as the primer, revealed products with the same 5′ ends at G-1147 and G-1180 observed in YEpR5-pG-derived poly(A)$^-$ RNA (not shown). These results provide additional support for our conclusion that degradation of the two transcripts is initiated by specific endonucleolytic cleavage within a limited target region located between approximately positions 1100 and 1200, that the resulting fragments are subsequently degraded exonucleolytically in the 5′→3′ direction, and that a poly(G) tract form considerably retards this degradation.

Accumulation of the 5′-terminal degradation intermediate does not depend upon inhibition of translation. As shown previously (60), insertion of a poly(G) tract into the 5′-UTR of a *PGK1* transcript inhibits its translation almost completely, most likely by blocking access of ribosomes to the AUG start codon. Since the stability of *PGK1* mRNA as a whole is increased in yeast cells treated with the translational inhibitor cycloheximide (19), we wanted to ascertain whether the accumulation of the 5′-terminal degradation intermediate of the *PGK1*-pGpG transcript is due to its inability to be translated. Rather than using cycloheximide, which "freezes" ribosomes on the mRNA and may also block the production of a labile component of the degradative machinery (19), we used plasmid dINpCpG. This plasmid is identical to dINpGpG except that it contains a poly(C)$_{18}$ instead of a poly(G)$_{18}$ insertion in the 5′-UTR of the *PGK1* gene (Fig. 1). The translational efficiency of the *PGK1*-pCpG mutant mRNA is only about 20% of that of its wild-type counterpart (60). Figure 10 shows Northern blots of total RNA from exponentially growing dINpCpG-transformed Y260 cells, analyzed with the *Eco*RI-*Cla*I probe corresponding to the *PGK1* coding region (Fig. 10A) or the 3′-UTR-specific TPGK probe (Fig. 10B). While the 3′-terminal degradation intermediate is clearly visible in the latter autoradiograph, no trace of the 5′-terminal intermediate can be detected in the blot probed with the fragment covering the *PGK1* coding region. This finding shows that a severe reduction in translatability of the *PGK1* transcript in itself is not sufficient to cause detectable accumulation of the 5′-terminal degradation intermediate.

Detection of cleavage sites in wild-type *PGK1* mRNA. All experiments mapping the endonucleolytic cleavage sites described so far were carried out on mutant forms of *PGK1* mRNA. To address the question of whether degradation of

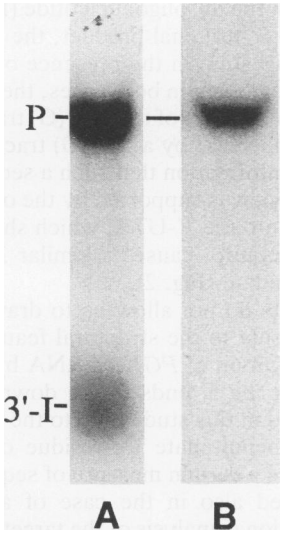

FIG. 10. Degradation intermediates of *PGK1*-pCpG mRNA. Total RNA was isolated from exponentially growing Y260 cells transformed with plasmid dINpCpG, carrying a poly(C) tract in the 5′-UTR and a poly(G) tract in the 3′-UTR (see Fig. 1). The RNA was analyzed by Northern hybridization with an excess of either the *Eco*RI-*Cla*I fragment of the *PGK1* gene, radiolabeled by random priming (A), or the 3′-UTR-specific TPGK oligonucleotide, radiolabeled at its 5′ end (B), as the probe. In each lane, 10 μg of RNA was used. The intact transcript and the 3′-terminal degradation intermediate are indicated by P and 3′-I, respectively.

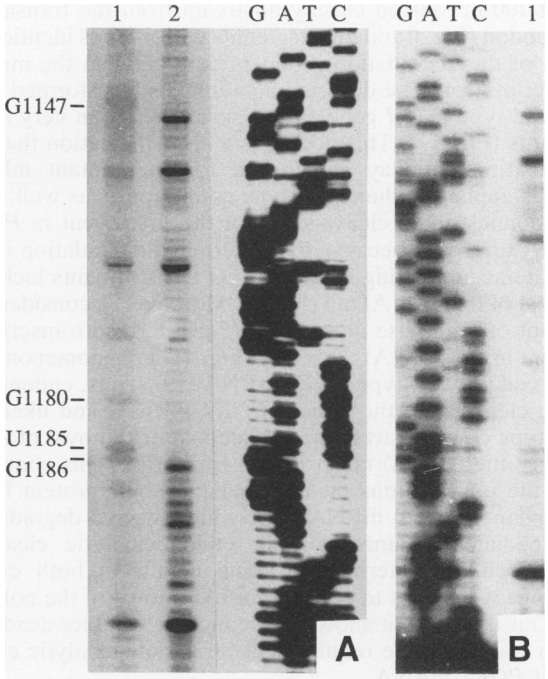

FIG. 11. Mapping of endonucleolytic cleavage positions in wild-type *PGK1* mRNA. (A) Total RNA was isolated from exponentially growing YEpR5-transformed Y260 cells, separated into the poly(A)$^+$ and poly(A)$^-$ fractions, and subjected to primer extension analysis with a deoxyoligonucleotide complementary to nt 1219 to 1238 of *PGK1* mRNA. Lanes: 1, poly(A)$^-$ RNA (20 μg); 2, poly(A)$^+$ RNA (1 μg). The sequence ladder (lanes G, A, T, and C) was obtained with the same primer. Lanes 1 and 2 represent an exposure of the autoradiogram five times longer than used for the sequence ladder. (B) Primer extension analysis of a synthetic *PGK1* mRNA fragment obtained by in vitro transcription of the *Kpn*I-*Sna*BI gene fragment (see Fig. 1) cloned under control of the bacteriophage T7 promoter of the pGEM3 vector (61) (lane 1). The same primer as used for panel A was used. The sequence ladder (lanes G, A, T, and C) was obtained with the same synthetic fragment.

wild-type *PGK1* mRNA follows the same pathway, we used *PGK1*-specific probes to carry out primer extension and S1 nuclease mapping experiments on poly(A)$^-$ RNA isolated from YEpR5-transformed Y260 cells, containing a high level of wild-type *PGK1* mRNA (59, 60). Two specific 5′ ends mapping at precisely the same positions as identified in the experiments with mutant *PGK1* mRNAs, namely, G-1180 and G-1147, were unequivocally detected, albeit only after very long exposure of the primer extension gel. In addition, specific 5′ ends were found at positions U-1185 and G-1186 (Fig. 11A, lane 1). The bands in question are absent from a reverse transcription analysis of poly(A)$^+$ RNA use as a control (Fig. 11A, lane 2). Conversely, the poly(A)$^+$ lane contains a number of bands that are absent from the poly(A)$^-$ lane or present at much reduced levels. However, reverse transcription analysis of a synthetically prepared *PGK1* mRNA fragment covering the same region (Fig. 11B) demonstrates that these bands are all artificial stops of the enzyme.

The reason for the appearance of additional specific 5′ ends at U-1185 and G-1186 in degradation products of the wild-type *PGK1* mRNA is not clear. We suggest that their presence may be due to a slightly different structure of the endonucleolytic target region in the wild-type transcript compared with its mutant counterparts. This view would be in agreement with the idea that the poly(G) insertion somehow retards the rate-limiting endonucleolytic cleavage by influencing the recognition of the target region by the enzyme. It should be noted that G-1186 again corresponds to the 3′-terminal residue of a 5′-GGUG-3′ motif (Fig. 7).

We were unable to detect any 3′ ends by S1 mapping of wild-type *PGK1* mRNA by using a probe that overlaps the endonucleolytic target region, even when we used fractionated poly(A)$^-$ RNA from YEpR5-transformed cells (Fig. 9, lanes 5 and 6). The close correspondence between the 5′ ends detected in the primer extension analysis of YEpR5-derived RNA and those detected in dINpGpG- and YEpR5-pG-derived transcripts strongly suggests, however, that the degradation pathway deduced above for the mutant *PGK1* mRNAs is not peculiar to these mutant transcripts but also applies to their wild-type counterparts.

DISCUSSION

A major handicap in elucidating the precise nature and order of events during decay of an mRNA is the fact that, as a rule, intermediates produced in the course of this process are extremely short-lived and therefore very difficult to detect and characterize. The experiments described in this report demonstrate that insertion of a poly(G) tract into the 5′- or 3′-UTR of yeast *PGK1* mRNA causes such degradation intermediates to accumulate to high levels in cells transformed with multiple copies of the mutant genes (Fig. 2 and 8). Characterization of these intermediates by S1 nuclease and primer extension analysis has allowed us to establish that the first attack on the actual body of the mutant *PGK1* transcripts is carried out by an endonuclease and is directed at specific sites within a relatively small target region of

about 100 nt located closely upstream from the translation stop codon (Fig. 6 and 9). Fragments with 5′ ends identical to those of the degradation products derived from the mutant transcripts could be detected also in cells transformed with the wild-type *PGK1* gene, albeit, as expected, in very small amounts (Fig. 11). This finding is a clear indication that the degradation pathway established for the mutant mRNA species applies to their wild-type counterparts as well.

Endonucleolytic cleavage is not the first event in *PGK1* mRNA turnover, because the 3′-terminal degradation intermediate accumulating in YEpR5-pG transformants lacks all or most of the poly(A) tail (Fig. 3). Moreover, a considerable amount of otherwise intact YEpR5-pG-derived transcript is present in the poly(A)$^-$ fraction (Fig. 4), a phenomenon also observed for wild-type *PGK1* mRNA (19). Thus, endonucleolytic cleavage of the mutant *PGK1* mRNA, and likely its wild-type counterpart as well, occurs after removal of all or most of the poly(A) tail from the transcript. This contrasts with the observations on mammalian apolipoprotein II (6) and avian 9E3 (56) mRNAs, for which in vivo degradation intermediates originating from endonucleolytic cleavage have been characterized in some detail. In both cases, cleavage was found to occur prior to removal of the poly(A) tail. Our data do not allow us to conclude whether deadenylation is an absolute requirement for endonucleolytic cleavage of *PGK1* mRNA.

While loss of the poly(A) tail precedes endonucleolytic cleavage, it is not the rate-limiting step in *PGK1* mRNA decay. The data presented in Fig. 5 show that the half-life of the poly(A) tail of both wild-type and YEpR5-pG-derived mutant *PGK1* transcripts is approximately 10 min, in close agreement with the figure derived previously for wild-type *PGK1* transcripts by Herrick et al. (19). This is well below the half-life of the wild-type and mutant transcripts as a whole (19, 62), which identifies the endonucleolytic cleavage in the 1100–1200 region as the rate-limiting step in their turnover. Inserting a poly(G) tract into the 3′-UTR of *PGK1* mRNA, thus, must reduce the rate of endonucleolytic cleavage, probably as the result of a conformational change in the mRNA. It remains to be seen whether this conformational change limits the accessibility of the target site to the enzyme or whether it directly affects higher-order structural features of the mRNA recognized by the endonuclease.

As is clear from the accumulation of deadenylated degradation intermediates extending to the transcription termination site in YEpR5-transformed cells (Fig. 4), removal of the poly(A) tail does not expose *PGK1* transcripts to 3′→5′ exonuclease activity, although such an activity has been detected in yeast cells (55). In fact, 3′→5′ exonuclease does not appear to play a role of any consequence in *PGK1* mRNA turnover, because insertion of a poly(G) tract immediately upstream from the AUG start codon effectively stabilizes the long 5′-terminal product of the endonucleolytic cleavage (Fig. 8 and 9). Therefore, we conclude that a 5′→3′ exonuclease(s) acts as the major scavenger of the products of the rate-limiting endonucleolytic cleavage of *PGK1* mRNA. Evidently, progression of the exonuclease is blocked by a poly(G) sequence, causing accumulation of the intermediates observed in YEpR5-pG and dINpGpG transformants. It is unlikely that exonucleolytic degradation of the 5′-terminal intermediate is linked to the translocation of ribosomes, since dINpCpG-transformed cells do not accumulate the 5′-terminal intermediate (Fig. 10) despite the fact that the *PGK1*-pCpG mRNA is very poorly translated (60).

We have not been able to map the 5′ end of either of the two degradation intermediates precisely. However, their hybridization with the dC oligonucleotide (Fig. 2 and 8) and, in the case of the 3′-terminal product, the reduction in size upon RNase H digestion in the presence of this oligonucleotide (Fig. 3) indicate that in both cases, the 5′ end is located at or very close to the start of the poly(G) tract. The blocking of the 5′→3′ exonuclease by a poly(G) tract is probably due to the peculiar conformation that such a sequence can adopt (18, 63, 68). This view is supported by the observation that a $G_{18}C_{18}$ insertion into the 3′-UTR, which should form a very stable hairpin structure, causes a similar 3′-terminal intermediate to accumulate (Fig. 2).

Our experiments do not allow us to draw definitive conclusions with respect to the structural features required for the specific recognition of *PGK1* mRNA by the endonuclease. The fact that the 5′ ends of the downstream cleavage products identified in this study map to the 3′-terminal G, or in one case the penultimate U, residue of a 5′-GGUG-3′ sequence indicates a certain measure of sequence specificity as has been noted also in the case of apolipoprotein II mRNA (6). Mutational analysis of the target region by means of an in vitro system from *S. cerevisiae* 20B-12 cells that mimics the in vivo endonucleolytic cleavage events supports this idea, since it showed that changing GGUG to GGUA abolished 5′-end formation at that particular sequence (61). However, it is also clear that more than just a GGUG motif is required, since the target region contains additional copies of this motif at which 5′ ends were not detected by primer extension analysis (Fig. 6). Furthermore, the 5′-terminal degradation intermediate accumulating in dINpGpG transformants still possesses nine GGUG sequences (20) that evidently do not serve as recognition sites for the endonuclease. Further mutational analysis and structure mapping of the target region will be required to determine the minimal requirements for its interaction with the endonuclease.

The endonuclease cleaving *PGK1* mRNA does not seem to correspond to either of the two yeast endoribonucleases that have so far been characterized in some detail. The enzyme described by Stevens (53) is highly specific for pyrimidine-A bonds, whereas our enzyme seems to cut preferentially at pyrimidine-G bonds. Mead and Oliver (36) have isolated a double-stranded yeast endoribonuclease which is Mg^{2+} independent and, in fact, is strongly inhibited by Mg^{2+} ions. Data obtained with the in vitro system mentioned above, however, indicate an absolute requirement for Mg^{2+} ions in the endonucleolytic cleavage of *PGK1* mRNA. While a Mg^{2+}-dependent endoribonuclease has been detected in yeast cells (30), the partially purified enzyme did not show any base specificity.

Stevens has also isolated a processive, Mg^{2+}-dependent 5′→3′ exonuclease from yeast cells that might correspond to the scavenging exonuclease revealed by our experiments (52, 55) except for the fact that its ionic requirements, in particular its inhibition by potassium ions, cannot be well reconciled with those of our in vitro system.

ACKNOWLEDGMENTS

We thank Victoria de Regt for excellent technical assistance during the initial phases of this work, Renske van der Veen for helpful suggestions, and J. Boesten for synthesizing the deoxyoligonucleotides used in this study. We gratefully acknowledge the continuous interest and support of R. J. Planta.

This work was supported in part by the Programmacommissie Industriële Biotechnologie, with financial aid from the Netherlands Ministry of Economic Affairs.

REFERENCES

1. **Atwater, J. A., R. Wisdom, and I. M. Verma.** 1990. Regulated mRNA stability. Annu. Rev. Genet. **24**:519–541.
2. **Barker, G. F., and K. Beemon.** 1991. Nonsense codons within the Rous sarcoma virus *gag* gene decrease the stability of unspliced viral RNA. Mol. Cell. Biol. **11**:2760–2768.
3. **Baserga, S. J., and E. J. Benz, Jr.** 1988. Nonsense mutations in the human β-globin gene affect mRNA metabolism. Proc. Natl. Acad. Sci. USA **85**:2056–2060.
4. **Belasco, J. G., and C. F. Higgins.** 1988. Mechanisms of mRNA decay in bacteria: a perspective. Gene **72**:15–23.
5. **Bernstein, P., S. W. Peltz, and J. Ross.** 1989. The poly(A)-poly(A)-binding protein complex is a major determinant of mRNA stability in vitro. Mol. Cell. Biol. **9**:659–670.
6. **Binder, R., S.-P. L. Hwang, R. Ratnasabapathy, and D. L. Williams.** 1989. Degradation of apolipoprotein II mRNA occurs via endonucleolytic cleavage at 5′-AAU-3′/5′-UAA-3′ elements in single-stranded loop domains of the 3′-noncoding region. J. Biol. Chem. **264**:16910–16918.
7. **Bohjanen, P. R., B. Petryniak, C. H. June, C. B. Thompson, and T. Lindsten.** 1991. An inducible cytoplasmic factor (AU-B) binds selectively to AUUUA multimers in the 3′ untranslated region of lymphokine messenger RNA. Mol. Cell. Biol. **11**: 3288–3295.
8. **Bouvet, P., J. Paris, M. Philippe, and H. B. Osborne.** 1991. Degradation of a developmentally regulated mRNA in *Xenopus* embryos is controlled by the 3′ region and requires the translation of another maternal mRNA. Mol. Cell. Biol. **11**:3115–3124.
9. **Brawerman, G.** 1989. mRNA decay: finding the right targets. Cell **57**:9–10.
10. **Brewer, G.** 1991. An A+U-rich element RNA-binding factor regulates c-*myc* messenger RNA stability in vitro. Mol. Cell. Biol. **11**:2460–2466.
11. **Brewer, G., and J. Ross.** 1989. Regulation of c-*myc* mRNA stability in vitro by a labile destabilizer with an essential nucleic acid component. Mol. Cell. Biol. **9**:1996–2006.
12. **Brown, A. J. P.** 1989. Messenger RNA stability in yeast. Yeast **5**:239–257.
13. **Caput, D., B. Beutler, K. Hartog, R. Thayer, S. Brown-Shimmer, and A. Cerami.** 1986. Identification of a common nucleotide sequence in the 3′-untranslated region of mRNA molecules specifying inflammatory mediators. Proc. Natl. Acad. Sci. USA **83**:1670–1674.
14. **Casey, J. L., D. M. Koeller, V. C. Ramin, R. D. Klausner, and J. B. Harford.** 1989. Iron regulation of transferrin receptor mRNA requires iron-responsive elements and a rapid turnover determinant in the 3′ untranslated region of the mRNA. EMBO J. **8**:3693–3699.
15. **Gay, D. A., S. S. Sisodia, and D. W. Cleveland.** 1989. Autoregulatory control of β-tubulin mRNA stability is linked to translation elongation. Proc. Natl. Acad. Sci. USA **86**:5763–5767.
16. **Gozalbo, D., and S. Hohmann.** 1990. Nonsense suppressors partially revert the decrease of the mRNA level of a nonsense mutant allele in yeast. Curr. Genet. **17**:77–79.
17. **Graves, R. A., N. B. Pandey, N. Chodchoy, and W. F. Marzluff.** 1987. Translation is required for histone mRNA degradation. Cell **48**:615–626.
18. **Henderson, E. R., C. C. Hardin, S. K. Walk, I. Tinoco, Jr., and E. H. Blackburn.** 1987. Telomeric DNA oligonucleotides form novel intramolecular structures containing guanine-guanine base pairs. Cell **51**:899–908.
19. **Herrick, D., R. Parker, and A. Jacobson.** 1990. Identification of stable and unstable mRNAs in *Saccharomyces cerevisiae*. Mol. Cell. Biol. **10**:2269–2284.
20. **Hitzeman, R. A., F. E. Hagie, J. S. Hayflick, C. Y. Chen, P. H. Seeburg, and R. Derynck.** 1982. The primary structure of the *Saccharomyces cerevisiae* gene for 3-phosphoglycerate kinase. Nucleic Acids Res. **10**:7791–7808.
21. **Hoekema, A., R. A. Kastelein, M. Vasser, and H. A. de Boer.** 1987. Codon replacement in the *PGK1* gene of *Saccharomyces cerevisiae*: experimental approach to study the role of biased codon usage in gene expression. Mol. Cell. Biol. **7**:2914–2924.
22. **Hwang, S.-P. L., M. Eisenberg, R. Binder, G. S. Shelness, and D. L. Williams.** 1989. Predicted structures of apolipoprotein II mRNA constrained by nuclease and dimethyl sulfate reactivity: stable secondary structures occur predominantly in local domains via intraexonic base pairing. J. Biol. Chem. **264**:8410–8418.
23. **Iwai, Y., M. Bickel, D. H. Pluznik, and R. B. Cohen.** 1991. Identification of sequences within the murine granulocyte-macrophage colony-stimulating factor messenger RNA 3′-untranslated region that mediate messenger RNA stabilization induced by mitogen treatment of EL-4 thymoma cells. J. Biol. Chem. **266**:17959–17965.
24. **Jäck, H.-M., J. Berg, and M. Wabl.** 1989. Translation affects immunoglobulin mRNA stability. Eur. J. Immunol. **19**:843–847.
25. **Jones, E.** 1976. Proteinase mutants of *Saccharomyces cerevisiae*. Genetics **85**:23–33.
26. **Kabnick, K. S., and D. E. Housman.** 1988. Determinants that contribute to cytoplasmic stability of human c-*fos* and β-globin mRNAs are located at several sites in each mRNA. Mol. Cell. Biol. **8**:3244–3250.
27. **Kennedy, I. M., J. K. Haddow, and J. B. Clements.** 1991. A negative regulatory element in the human papillomavirus type 16 genome acts at the level of late mRNA stability. J. Virol. **65**:2093–2097.
28. **Koeller, D. M., J. L. Casey, M. W. Hentze, E. M. Gerhardt, L.-N. L. Chan, R. D. Klausner, and J. B. Harford.** 1989. A cytosolic protein binds to structural elements within the iron regulatory region of the transferrin receptor mRNA. Proc. Natl. Acad. Sci. USA **86**:3574–3578.
29. **Laird-Offringa, I. A., C. L. de Wit, P. Elfferich, and A. J. van der Eb.** 1990. Poly(A)-tail shortening is the translation-dependent step in c-*myc* mRNA degradation. Mol. Cell. Biol. **10**: 6132–6140.
30. **Lee, S. V., Y. Nakao, and R. M. Bock.** 1968. The nucleases of yeast. II. Purification, properties and specificity of an endonuclease from yeast. Biochim. Biophys. Acta **151**:126–136.
31. **Leer, R. J., M. M. C. Van Ramsdonk-Duin, M. J. M. Hagendoorn, W. H. Mager, and R. J. Planta.** 1984. Structural comparison of yeast ribosomal protein genes. Nucleic Acids Res. **12**:6685–6700.
32. **Losson, R., and F. Lacroute.** 1979. Interference of nonsense mutations with eukaryotic messenger RNA stability. Proc. Natl. Acad. Sci. USA **76**:5134–5137.
33. **Malter, J. S.** 1989. Identification of an AUUUA-specific messenger RNA binding protein. Science **246**:664–666.
34. **Maniatis, T., E. F. Fritsch, and J. Sambrook.** 1982. Molecular cloning: a laboratory manual. Cold Spring Harbor Laboratory, Cold Spring Harbor, N.Y.
35. **Marzluff, W. F., and N. B. Pandey.** 1988. Multiple regulatory steps control histone mRNA concentrations. Trends Biochem. Sci. **13**:49–52.
36. **Mead, D. J., and S. G. Oliver.** 1983. Purification and properties of a double-stranded ribonuclease from the yeast *Saccharomyces cerevisiae*. Eur. J. Biochem. **137**:501–507.
37. **Minvielle-Sebastia, L., B. Winsor, N. Bonneaud, and F. Lacroute.** 1991. Mutations in the yeast *RNA14* and *RNA15* genes result in an abnormal messenger RNA decay rate: sequence analysis reveals an RNA-binding domain in the RNA15 protein. Mol. Cell. Biol. **11**:3075–3087.
38. **Müllner, E. W., and L. C. Kühn.** 1988. A stem-loop in the 3′ untranslated region mediates iron-dependent regulation of transferrin receptor mRNA stability in the cytoplasm. Cell **53**:815–825.
39. **Müllner, E. W., B. Neupert, and L. C. Kühn.** 1989. A specific mRNA binding factor regulates the iron-dependent stability of cytoplasmic transferrin receptor mRNA. Cell **58**:373–382.
40. **Munroe, D., and A. Jacobson.** 1990. Tales of poly(A): a review. Gene **91**:151–158.
41. **Nonet, M., C. Scafe, J. Sexton, and R. Young.** 1987. Eukaryotic RNA polymerase conditional mutant that rapidly ceases mRNA synthesis. Mol. Cell. Biol. **7**:1602–1611.
42. **Pandey, N. B., and W. F. Marzluff.** 1987. The stem-loop structure at the 3′-end of histone mRNA is necessary and

sufficient for regulation of histone mRNA stability. Mol. Cell. Biol. **7**:4557–4559.
43. **Parker, R., and A. Jacobson.** 1990. Translation and a 42-nucleotide segment within the coding region of the mRNA encoded by the *MATa1* gene are involved in promoting rapid mRNA decay in yeast. Proc. Natl. Acad. Sci. USA **87**:2780–2784.
44. **Pelsy, F., and F. Lacroute.** 1984. Effect of ochre nonsense mutations on yeast *URA1* stability. Curr. Genet. **8**:277–282.
45. **Peltz, S. W., and J. Ross.** 1987. Autogenous regulation of histone mRNA decay by histone proteins in a cell free system. Mol. Cell. Biol. **7**:4345–4356.
46. **Peppel, K., J. M. Vinci, and C. Baglioni.** 1991. The AU-rich sequences in the 3′ untranslated region mediate the increased turnover of interferon mRNA induced by glucocorticoids. J. Exp. Med. **173**:349–355.
47. **Petersen, D. D., S. R. Koch, and D. K. Granner.** 1989. 3′ Noncoding region of phosphoenolpyruvate carboxykinase mRNA contains a glucocorticoid-responsive mRNA-stabilizing element. Proc. Natl. Acad. Sci. USA **86**:7800–7804.
48. **Ross, J.** 1989. The turnover of messenger RNA. Sci. Am. **260**:28–35.
49. **Shaw, G., and R. Kamen.** 1986. A conserved AU sequence from the 3′-untranslated region of GM-CSF mRNA mediates selective mRNA degradation. Cell **46**:659–667.
50. **Shyu, A.-B., J. G. Belasco, and M. E. Greenberg.** 1991. Two distinct destabilizing elements in the c-*fos* message trigger deadenylation as a first step in rapid mRNA decay. Genes Dev. **5**:221–231.
51. **Soloway, P. D., and T. Shenk.** 1990. The adenovirus type 5 I-leader open reading frame functions in *cis* to reduce the half-life of L1 mRNAs. J. Virol. **64**:551–558.
52. **Stevens, A.** 1980. Purification and characterization of a *Saccharomyces cerevisiae* exoribonuclease which yields 5′-mononucleotides by a 5′→3′ mode of hydrolysis. J. Biol. Chem. **255**:3080–3085.
53. **Stevens, A.** 1985. Pyrimidine-specific cleavage by an endoribonuclease of *Saccharomyces cerevisiae*. J. Bacteriol. **164**:57–62.
54. **Stevens, A.** 1986. Novel specificity of an endoribonuclease of yeast. FEBS Lett. **205**:210–214.
55. **Stevens, A., and M. K. Maupin.** 1987. A 5′→3′ exoribonuclease of *Saccharomyces cerevisiae*: size and novel substrate specificity. Arch. Biochem. Biophys. **252**:339–347.
56. **Stoeckle, M. Y., and H. Hanafusa.** 1989. Processing of 9E3 mRNA and regulation of its stability in normal and Rous sarcoma virus-transformed cells. Mol. Cell. Biol. **9**:4738–4745.
57. **Theil, E. C.** 1990. Regulation of ferritin and transferrin receptor mRNAs. J. Biol. Chem. **265**:4771–4774.
58. **Vakalopoulou, E., J. Schaack, and T. Shenk.** 1991. A 32-kilodalton protein binds to AU-rich domains in the 3′ untranslated regions of rapidly degraded mRNAs. Mol. Cell. Biol. **11**:3355–3364.
59. **Van den Heuvel, J. J., R. J. M. Bergkamp, R. J. Planta, and H. A. Raué.** 1989. Effect of deletions in the 5′-noncoding region on the translational efficiency of phosphoglycerate kinase mRNA in yeast. Gene **79**:83–95.
60. **Van den Heuvel, J. J., R. J. Planta, and H. A. Raué.** 1990. Effect of leader primary structure on the translational efficiency of phosphoglycerate kinase mRNA in yeast. Yeast **6**:473–482.
61. **Vreken, P., N. Buddelmeijer, and H. A. Raué.** Nucleic Acids Res., in press.
62. **Vreken, P., R. van der Veen, V. C. H. F. de Regt, A. L. de Maat, R. J. Planta, and H. A. Raué.** 1991. Turnover rate of yeast PGK mRNA can be changed by specific alterations in its trailer structure. Biochimie **73**:729–737.
63. **Williamson, J. R., M. K. Raghuraman, and T. R. Cech.** 1989. Monovalent cation-induced structure of telomeric DNA: the G-quartet model. Cell **59**:871–880.
64. **Wisdom, R., and W. Lee.** 1991. The protein-coding region of c-*myc* mRNA contains a sequence that specifies rapid mRNA turnover and induction by protein synthesis inhibitors. Genes Dev. **5**:232–243.
65. **Xu, H. X., L. Johnson, and M. Grunstein.** 1990. Coding and noncoding sequences at the 3′ end of yeast histone H2B mRNA confer cell cycle regulation. Mol. Cell. Biol. **10**:2687–2694.
66. **Yen, T. J., D. A. Gay, J. S. Pachter, and D. W. Cleveland.** 1988. Autoregulated changes in stability of polyribosome-bound β-tubulin mRNAs are specified by the first 13 translated nucleotides. Mol. Cell. Biol. **8**:1224–1235.
67. **Yen, T. J., P. S. Machlin, and D. W. Cleveland.** 1988. Autoregulated instability of β-tubulin mRNAs by recognition of the nascent amino terminus of β-tubulin. Nature (London) **334**:580–585.
68. **Zimmerman, S. B., G. H. Cohen, and D. R. Davies.** 1975. X-ray fiber diffraction and model-building study of polyguanylic acid and polyinosinic acid. J. Mol. Biol. **92**:181–192.
69. **Zitomer, R. S., D. L. Montgomery, D. L. Nichols, and B. D. Hall.** 1979. Transcriptional regulation of the yeast cytochrome *c* gene. Proc. Natl. Acad. Sci. USA **76**:3627–3631.
70. **Zucker, M., and P. Stiegler.** 1981. Optimal computer folding of large RNA sequences using thermodynamics and auxiliary information. Nucleic Acids Res. **9**:133–148.